

Exponentially Enhanced Non-Hermitian Cooling

Haowei Xu¹, Uroš Delić^{2,3}, Guoqing Wang^{1,3}, Changhao Li^{1,3}, Paola Cappellaro^{1,3,4,*} and Ju Li^{1,5,†}

¹Department of Nuclear Science and Engineering, Massachusetts Institute of Technology, Cambridge, Massachusetts 02139, USA

²University of Vienna, Faculty of Physics, Vienna Center for Quantum Science and Technology, A-1090 Vienna, Austria

³Research Laboratory of Electronics, Massachusetts Institute of Technology, Cambridge, Massachusetts 02139, USA

⁴Department of Physics, Massachusetts Institute of Technology, Cambridge, Massachusetts 02139, USA

⁵Department of Materials Science and Engineering, Massachusetts Institute of Technology, Cambridge, Massachusetts 02139, USA

 (Received 15 September 2023; accepted 14 February 2024; published 15 March 2024)

Certain non-Hermitian systems exhibit the skin effect, whereby the wave functions become exponentially localized at one edge of the system. Such exponential amplification of wavefunction has received significant attention due to its potential applications in, e.g., classical and quantum sensing. However, the opposite edge of the system, featured by exponentially *suppressed* wave functions, remains largely unexplored. Leveraging this phenomenon, we introduce a non-Hermitian cooling mechanism, which is fundamentally distinct from traditional refrigeration or laser cooling techniques. Notably, non-Hermiticity will not amplify thermal excitations, but rather redistribute them. Hence, thermal excitations can be cooled down at one edge of the system, and the cooling effect can be *exponentially* enhanced by the number of auxiliary modes, albeit with a lower bound that depends on the dissipative interaction with the environment. Non-Hermitian cooling does not rely on intricate properties such as exceptional points or nontrivial topology, and it can apply to a wide range of excitations.

DOI: [10.1103/PhysRevLett.132.110402](https://doi.org/10.1103/PhysRevLett.132.110402)

Introduction.—Non-Hermiticity arises naturally in open quantum systems. Prototypical examples are loss and gain, which were often considered nuisances in standard Hermitian quantum mechanics. Recently it was realized that a careful balance between gain and loss can lead to the emergence of intriguing phenomena such as parity-time symmetry breaking and exceptional points [1–5]. Other non-Hermitian phenomena, such as non-Hermitian topology [6–11], which can be defined solely based on eigenvalues instead of eigenvectors, have generated considerable attention as well.

A particularly interesting property of certain non-Hermitian systems is the non-Hermitian skin effect (NHSE) [12–19], whereby the wave functions are exponentially localized at one boundary of the system. Various novel applications have been proposed based on the NHSE, such as directional amplification of signals [20–23] and (potentially exponentially) enhanced sensing [24–26]. However, the majority of studies in non-Hermitian physics focus on non-Hermiticity-induced *amplification* [1–4,20–28,15]. It is worth noting that the exponential amplification of wavefunctions on one edge implies the exponential *suppression* of wave functions on the opposite edge. This property, however, remains largely unexplored. In this work, we focus on applications of this effect in non-Hermitian systems, in particular toward cooling thermal excitations.

Cooling down thermal excitations is an essential step for numerous applications that span nearly all scientific and technological domains. However, traditional refrigeration

often requires bulky devices, and it can be rather difficult to cool down below certain limits, such as several milli-Kelvin in dilution refrigerators [29]. Meanwhile, laser cooling relies on relatively weak nonlinear optical processes [30–33], necessitating strong pumping lasers that can potentially result in side effects. A critical observation is that in both traditional refrigeration and laser cooling, cooling is achieved by transferring thermal excitations to auxiliary modes (thermal bath) that have *smaller* occupation numbers [Figs. 1(a) and 1(b)]. This raises the question: is this a necessary condition for cooling?

In this Letter, we propose a non-Hermitian cooling mechanism, which is related to nonreciprocal refrigeration [34,35],

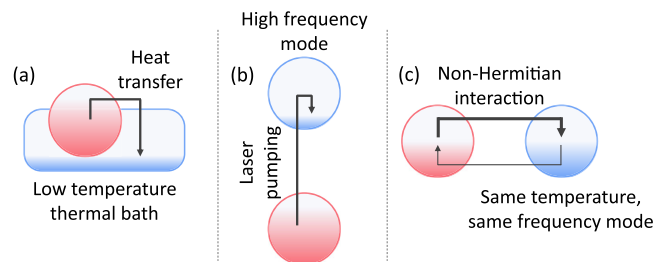


FIG. 1. Illustration of the mechanism of (a) traditional refrigeration, (b) laser cooling, and (c) non-Hermitian cooling. Red (blue) circles denote the principal (auxiliary) mode, and the color filling denotes thermal occupation. The arrows indicate the transfer of thermal excitation, with thicker arrows corresponding to faster transfer.

but is fundamentally different from traditional refrigeration or laser cooling. The non-Hermitian cooling stems from the *directional* transport of thermal excitations and can be achieved even if the auxiliary modes have the same occupation number [Fig. 1(c)]. We will demonstrate that directional transport does not significantly amplify but only redistributes thermal excitations in non-Hermitian systems. This guarantees that the localization of thermal excitation and heating on one edge (i.e., NHSE) will at the same time result in cooling on the opposite edge. By employing two different theoretical approaches, we reveal that the cooling effect can be exponentially enhanced by the number of auxiliary non-Hermitian modes, although a lower bound emerges when the dissipative interaction with the environment is included.

The non-Hermitian cooling is inherently versatile. In principle, it applies to various types of excitations including photons, phonons, magnons, etc. The non-Hermitian cooling does not require intricate properties such as parity-time symmetry [1,36–38], exceptional points [1–5], or nontrivial topologies [15,25,26]. The only requirement is the nonreciprocal hopping and directional transport of the excitations, corresponding to the emergence of the NHSE. Hence, we expect non-Hermitian cooling to be widely applicable.

In the following, we will first explain the distinctiveness of non-Hermitian cooling by comparing it with traditional refrigeration and laser cooling methods. Then, starting from two-mode systems, we will demonstrate the performance of non-Hermitian cooling, including the exponential enhancement in multi-mode systems, as well as the lower bound of the cooling effect. Finally, we will discuss some issues relevant to the practical realization of non-Hermitian cooling.

Traditional refrigeration, laser cooling, and non-Hermitian cooling.—For clarity, we will use principal and auxiliary to denote the mode to be cooled down and the modes that facilitate the cooling process, respectively. For traditional refrigeration, the key step is to attach the principal mode to the auxiliary modes (thermal bath) with the same intrinsic frequency but lower temperature, which have smaller occupation numbers. Then, the thermal excitations would naturally flow into the thermal bath via heat transfer, leading to the cooling effect [Fig. 1(a)]. Clearly, the lowest achievable temperature is the temperature of the thermal bath. While diverse schemes have been devised to create thermal baths with low temperatures, it can be extremely demanding and costly for traditional refrigeration to go beyond a certain limit, e.g., several millikelvin in dilution refrigerators [29].

Laser cooling uses a different mechanism. A low-frequency principal mode is coupled to an auxiliary mode with a higher (usually optical) frequency, whose effective thermal occupation is much smaller even at elevated temperatures [Fig. 1(b)]. It is worth noting that some other processes, such as dynamic nuclear polarization [39], employ a similar mechanism. For laser cooling, the thermal excitations in the principal mode are pumped to the

auxiliary mode by an external laser, which compensates for the energy difference. While laser cooling is remarkably successful, as seen in the achievement of picokelvin temperatures for ultracold atoms [40], it is ultimately limited by the laser power and the dissipation of the principal and auxiliary modes. Specifically, the transfer of thermal excitations via laser pumping relies on intrinsically weak and usually nonlinear optical processes. Hence, strong pumping lasers are required, which can cause heating and damage to the surrounding, especially in solid-state systems. Moreover, the auxiliary high-frequency modes usually have high dissipation rates, which also limits the effectiveness of laser cooling.

One can see that both traditional refrigeration and laser cooling result from transferring thermal excitations to auxiliary modes with smaller occupation numbers. Indeed, for bosonic modes, the transition (energy transfer) rate for both traditional contact cooling and laser cooling from the principal to the auxiliary mode is $gn_1(1+n_2)$, while that in the reverse direction is $gn_2(1+n_1)$, so the net flow is $g(n_1-n_2)$. Here n_1 (n_2) is the occupation number of the principal (auxiliary) mode, while g is the reciprocal coupling strength. Clearly, cooling of the principal mode requires $n_2 < n_1$. Similar analyses hold for fermionic modes as well.

In contrast, this is not a necessary condition for cooling in a non-Hermitian system. Even if the principal and auxiliary modes have the same occupation number, cooling could still be achieved if (i) the transfer of excitations is directional, so that the excitations preferably jump from the principal to the auxiliary modes [Fig. 1(c)]; (ii) the directional transport does not significantly amplify total thermal excitations in the system. In the following, we will demonstrate that both conditions can be satisfied in certain non-Hermitian systems.

Non-Hermitian cooling in two-mode systems.—To better understand the non-Hermitian cooling effect, let us first examine a two-mode system, where the principal mode-1 and auxiliary mode-2 have the same intrinsic frequency ω_0 [inset of Fig. 2(b)]. We will assume the two modes to be bosons, such as photons, phonons, or magnons, but the discussions below can be adapted to fermionic modes as well. We will show that in a non-Hermitian system, the transition rate from modes 1 to 2 can be different from that in the reverse direction, resulting in an unbalanced steady-state occupation (SSO) and an effective cooling effect. We consider the following Hamiltonian of the two-mode system in the rotating frame of ω_0

$$\mathcal{H} = t_{12}a_1a_2^\dagger + t_{21}a_1^\dagger a_2. \quad (1)$$

Here a_i (a_i^\dagger) is the annihilation (creation) operator of mode- i , while $t_{12} = te^A$ and $t_{21} = te^{-A}$ are the intermode coupling strength. The interaction is non-Hermitian when A has a nonzero real part. For definiteness and without loss

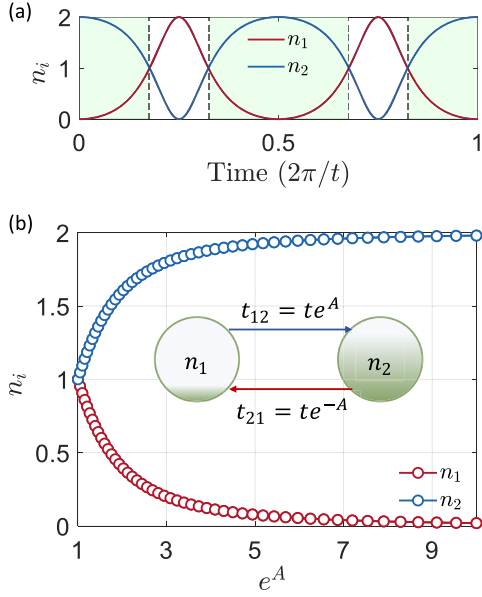


FIG. 2. (a) Unbalanced “Rabi” oscillation in the non-Hermitian two-mode system with $e^A = 2$. Green and white shaded regions correspond to $n_1 < n_2$ and $n_1 > n_2$, respectively. (b) Steady-state occupation as a function of e^A with $\kappa_1 = \kappa_2 = 0.01 t$. Inset of (b): Illustration of a non-Hermitian two-mode system. The color filling denotes SSO.

of generality, we will take $A > 0$ as a real number unless explicitly stated. The time evolution of the density matrix ρ can be described by the quantum master equation [41–43], $(\partial\rho/\partial t) = -i(\mathcal{H}\rho - \rho\mathcal{H}^\dagger) + i\text{Tr}\{\rho(\mathcal{H} - \mathcal{H}^\dagger)\}\rho + \sum_i \mathcal{L}(o_i)\rho$, which is adapted for a non-Hermitian Hamiltonian $\mathcal{H} \neq \mathcal{H}^\dagger$ (see Sec. 1 of Ref. [44] for detailed discussions, which also includes Refs. [8,14,21,41,45–47]). The dissipative interactions with the environment (thermal bath) are described by the Lindblad operators $\mathcal{L}(o_i)\rho \equiv o_i\rho o_i^\dagger - \frac{1}{2}(o_i^\dagger o_i\rho + \rho o_i^\dagger o_i)$ for operator o_i .

One can readily observe that when the dissipative interactions with the thermal bath are ignored, the “Rabi” oscillation between modes 1 and 2 is still periodic, but will deviate from a normal sinusoidal function [Fig. 2(a)]. Compared with the $1 \rightarrow 2$ oscillation, the reverse $2 \rightarrow 1$ oscillation takes a longer time $\tau_{21} \sim (1/t_{21})$, resulting in an unbalance between the two modes, and the excitations would preferably reside in mode 2.

Considering the dissipative interactions with the thermal bath and assuming the occupation numbers to be small, one has (Sec. 1 of Ref. [44])

$$\begin{aligned} \frac{\partial n_1}{\partial t} &\approx i[t_{12}\langle a_1 a_2^\dagger \rangle - t_{21}\langle a_1^\dagger a_2 \rangle] - \kappa_1[n_1 - n_{\text{th}}], \\ \frac{\partial \langle a_1^\dagger a_2 \rangle}{\partial t} &\approx i[t_{21}^* \langle a_2^\dagger a_2 \rangle - t_{12}\langle a_1^\dagger a_1 \rangle] - \frac{\kappa_1 + \kappa_2}{2} \langle a_1^\dagger a_2 \rangle. \end{aligned} \quad (2)$$

Here κ_i is the dissipation rate of mode i , and n_{th} is the occupation number of the thermal bath, which is assumed

to be the same for the two modes. Note that n_{th} is also the equilibrium occupation number of the two modes if the non-Hermiticity is absent (i.e., $t_{12} = t_{21}$). Meanwhile, $\langle o \rangle \equiv \text{Tr}\{\rho o\}$ indicates the thermal average of operator o , and $n_1 \equiv \langle a_1^\dagger a_1 \rangle$ is the occupation of mode 1. Similar equations hold when modes 1 and 2 are exchanged. In the steady state, one has

$$\begin{aligned} g_{12}n_1 + \kappa_1 n_1 &\approx g_{21}n_2 + \kappa_1 n_{\text{th}}, \\ g_{21}n_2 + \kappa_2 n_2 &\approx g_{12}n_1 + \kappa_2 n_{\text{th}}, \end{aligned} \quad (3)$$

where $g_{ij} = 2(|t_{ij}|^2 + t_{ij}t_{ji})/(\kappa_i + \kappa_j)$ is the non-Hermitian transition rate from mode i to j . Note that one recovers $g_{ij} = 4t^2/(\kappa_i + \kappa_j)$ for $A = 0$, which is a well-known result obtained from Fermi’s golden rule, if assuming Lorentzian lineshapes.

The SSO n_1 and n_2 as a function of e^A are shown in Fig. 2(b), where we assume $\kappa_1 = \kappa_2 = 0.01 t$ and $n_{\text{th}} = 1$. In a Hermitian system with $A = 0$, one has $n_1 = n_2 = n_{\text{th}}$, as expected. In contrast, one has $n_1 < n_{\text{th}}$ for $A > 0$, which is the non-Hermitian cooling effect. Moreover, n_1 gradually decreases to zero as e^A increases. Nonetheless, for finite values of e^A , the cooling effect is limited. For example, one has $n_1 \approx 0.4 n_{\text{th}}$ when $e^A = 2$. Note that this cooling effect is closely related to nonreciprocal refrigeration [34,35].

Exponential non-Hermitian cooling in multimode systems.—The cooling effect described in the previous section can be exponentially enhanced if more auxiliary modes are added. Ideally, one should be able to achieve $n_1 \propto (g_{12}/g_{21})^{-N}$ in an N -mode non-Hermitian chain [Fig. 3(a)]. The Hamiltonian of the chain in the rotating

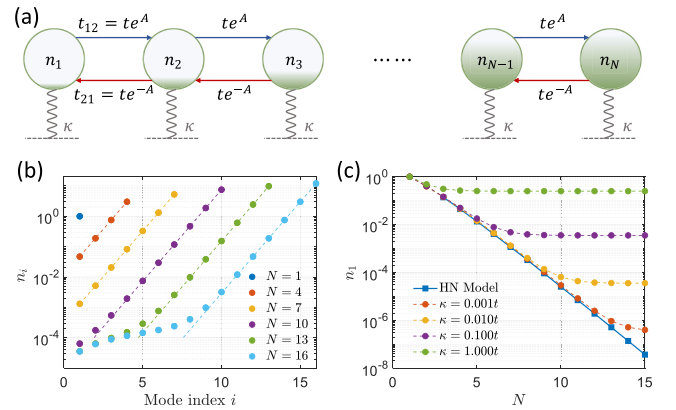


FIG. 3. (a) Illustration of a non-Hermitian N -mode chain. The color filling denotes SSO. (b) SSO of each mode in the chain with varying length N . The dashed line indicates the exponential scaling of $n_i \propto (g_{12}/g_{21})^{N-i}$. (c) SSO of the leftmost mode-1 as a function of N with varying κ . The solid blue line comes from Eq. (5), which coincides with the case of $\kappa \rightarrow 0$. We set $e^A = 2$ in (b),(c) and $\kappa = 0.01 t$ in (b).

frame is

$$\mathcal{H} = \sum_{i=1}^{N-1} t_{i,i+1} a_i a_{i+1}^\dagger + t_{i+1,i} a_i^\dagger a_{i+1}, \quad (4)$$

with $t_{i,i+1} = te^A$ and $t_{i+1,i} = te^{-A}$. This is the renowned non-Hermitian Hatano-Nelson model [12,18]. By diagonalizing Eq. (4), one has $\mathcal{H}|\psi_\alpha\rangle = \epsilon_\alpha|\psi_\alpha\rangle$, where the α th eigenstate has energy ϵ_α and right eigenvector $|\psi_\alpha\rangle$. Under the current setting, \mathcal{H} can be mapped to a Hermitian Hamiltonian by a similarity transformation [8,48]. Consequently, ϵ_α are all real numbers, while $|\psi_\alpha\rangle$ are exponentially localized on the right boundary, i.e., $\psi_\alpha^i \approx e^A \psi_\alpha^{i-1}$, which is the NHSE [8,18]. In many scenarios, the coupling strengths $te^{\pm A}$ are much smaller than other energy scales, such as the intrinsic mode frequency ω_0 and the temperature T . Hence, if one arbitrarily applies standard thermodynamics to the Hatano-Nelson model [49], then all the eigenstates $|\psi_\alpha\rangle$ should have almost the same probability to be occupied, and the SSO of the i th mode is

$$n_i^{\text{HN}} = n_{\text{th}} \sum_{\alpha} |\psi_\alpha^i|^2. \quad (5)$$

Here the superscript HN indicates that the occupations are obtained directly from the wavefunctions of the Hatano-Nelson model. One can easily verify that $n_i = n_{\text{th}}$ if the Hamiltonian is Hermitian ($A = 0$), as expected. In contrast, with $A > 0$, the NHSE implies that the SSO on the left edge is exponentially suppressed with $n_i^{\text{HN}} \approx e^{-2A} n_{i+1}^{\text{HN}}$ and $n_1^{\text{HN}} \sim n_{\text{th}} e^{-2NA}$, corresponding to the exponential cooling effect.

One may wonder whether the exponential cooling effect described above can survive if the dissipative interactions with the environment are incorporated. Fortunately, the answer is yes, although a lower bound on n_1 would arise with given e^A and κ . Generalizing the steady-state equations Eq. (3) to the N -mode system, one has

$$g_{i,i+1} n_i + g_{i,i-1} n_i + \kappa n_i = g_{i+1,i} n_{i+1} + g_{i-1,i} n_{i-1} + \kappa n_{\text{th}}, \quad (6)$$

$$i = 1, 2, \dots, N,$$

where for simplicity, we assume the thermal dissipation rate (κ) and the thermal bath occupation (n_{th}) to be the same for all modes. Meanwhile, we set $g_{i,i+1} = g_{12}$ and $g_{i+1,i} = g_{21}$, and the open boundary condition is implicitly incorporated by setting $g_{01} = g_{10} = g_{N,N+1} = g_{N+1,N} = 0$.

An intriguing and important observation from Eq. (6) is that the sum of SSO on all modes remains a constant, i.e., $\sum_i n_i \equiv N n_{\text{th}}$, regardless of the values of g_{ij} . This implies that an increase in the SSO of some modes must be accompanied by a decrease in other modes. While the thermal excitations can internally redistribute in different modes, the N -mode system as a whole must exhibit $N n_{\text{th}}$

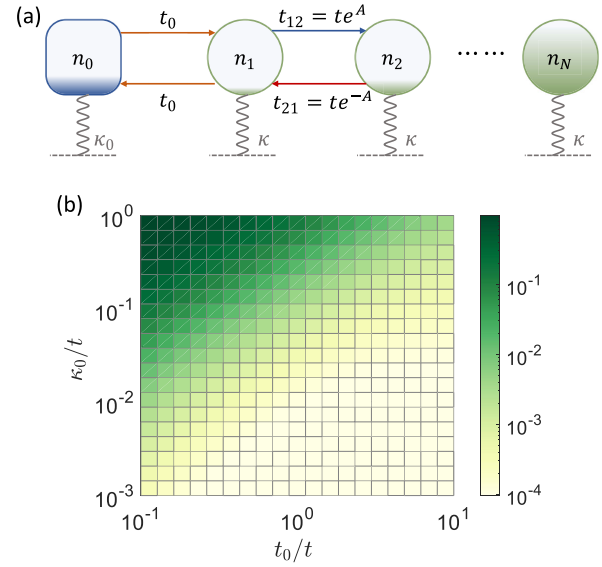


FIG. 4. (a) A Hermitian principal mode-0 is attached to the non-Hermitian chain. (b) SSO of mode-0 as a function of κ_0 and t_0 . The non-Hermitian chain has $N = 15$ modes with $e^A = 2$ and $\kappa = 0.01 t$.

excitations to the environment. This should be compared with the cases whereby an input signal is amplified by the non-Hermitian chain [20–22], which can be used to improve classical and/or quantum sensing [25,26]. Here, the non-Hermitian chain does not amplify but only redistributes the thermal excitations. This crucial property guarantees that the NHSE will lead to exponential non-Hermitian cooling.

We numerically solve the steady-state equations Eq. (6) to obtain the SSO in a non-Hermitian chain [Figs. 3(b) and 3(c)]. e^A is set to 2 unless explicitly stated. With a fixed and finite κ , the SSO of the leftmost mode n_1 first decreases exponentially with N , and then becomes a constant $\lim_{N \rightarrow \infty} n_1(\kappa, N) \approx [\kappa^2 n_{\text{th}} / (\kappa^2 + t_{12}^2 - t_{21}^2)]$ (Sec. 2 of Ref. [44]). While obtained using a different approach, n_1^{HN} in Eq. (5) coincides with the case of $\kappa \rightarrow 0$, i.e., $n_1^{\text{HN}} \approx \lim_{\kappa \rightarrow 0} n_1(\kappa, N)$. This agreement suggests that the theoretical results presented here should be robust. The nonreciprocal cooling studied in Refs. [34,35] corresponds to the special case of $N = 2$ in the current work. We would like to emphasize that using a multimode system ($N > 2$) can further reduce the lowest achievable occupation number n_1 of the principal mode.

Cooling down a reciprocally coupled mode.—In some situations, establishing a non-Hermitian interaction can be challenging, and/or can lead to unwanted side effects for the principal mode, such as extra dissipations [45]. In this case, one can attach the principal mode (denoted by 0 here) to mode 1 in the non-Hermitian chain described above. The interaction between modes 0 and 1, $\mathcal{H}_0 = t_0(a_0 a_1^\dagger + a_0^\dagger a_1)$, can be Hermitian [Fig. 4(a)]. The cooling

effect of mode 0 comes from the fact of $n_1 \ll n_{\text{th}}$, as the flow of thermal excitation will be dominantly in the $0 \rightarrow 1$, rather than the $1 \rightarrow 0$ direction, even if the transition between modes 0 and 1 is reciprocal. Using the steady-state equations Eq. (6), one can obtain the SSO [Fig. 4(b)]

$$n_0 \approx \frac{g_0 n_1 + \kappa_0 n_{\text{th}}}{g_0 + \kappa_0}, \quad (7)$$

where κ_0 is the dissipation rate of mode 0, and $g_0 = 4|t_0|^2/(\kappa + \kappa_0)$ is the reciprocal transition rate between mode 0 and 1. One can see that a cooling effect ($n_0 < n_{\text{th}}$) can be realized whenever $n_1 < n_{\text{th}}$.

Discussions.—The non-Hermitian cooling efficiency depends on two parameters, namely, e^A and κ/t . In theory, one can achieve $e^A \rightarrow \infty$ by judiciously designing the interaction between the two modes using, e.g., reservoir engineering [45] or parametric driving [21,46]. In practice, $e^A \gtrsim 3$ has been realized in, e.g., Josephson junctions [20], optomechanical circuits [50], and optically levitated nanoparticles [51]. Hence, we believe $e^A = 2$ used in this work is feasible. The non-Hermitian interaction between multiple modes has been demonstrated as well [52]. Still, additional experimental efforts are required to further increase e^A and N , so that the potential of the non-Hermitian cooling effect can be fully exploited. A concern can arise from the possible detrimental influence of thermal fluctuations in the external modes or driving fields that are used to induce the non-Hermitian interactions. Fortunately, our analyses show that the influence of such thermal fluctuations should be negligible in generating the non-Hermitian dynamics, at least in the first order approximation (Sec. 4 of Ref. [44]). Moreover, in practice the non-Hermitian interactions are often driven by optical photons [51,53], whose thermal fluctuations are extremely small because of their high intrinsic frequencies. Furthermore, strong couplings ($\kappa/t \ll 1$) can be realized between microwave resonators [54], mechanical resonators [55], magnons [56,57], etc. It should be emphasized that the coupling t here can be direct linear interactions without external pumping, such as the Zeeman interaction between magnons and microwave resonators. In contrast, for laser cooling the interactions between the principal and auxiliary modes are relatively weak (nonlinear) optical processes under external laser pumping, which leads to some limitations discussed before.

The presented non-Hermitian cooling applies to various excitations, including atoms, photons [15,58], phonons [17,50,59,60], Josephson circuits [20,21], magnons [42,61], etc., whereby non-Hermitian interactions have been realized. Moreover, non-Hermitian cooling exists whenever the wave function density is suppressed in certain local regions (not necessarily on the edge) of the non-Hermitian system. It does not require sophisticated properties such as exceptional points [1–5], nontrivial topology [15,26], or mixing between different quadratures of

the electromagnetic fields [25]. As an example, we investigated the non-Hermitian Su-Schrieffer-Heeger model (Bosonic) (Sec. 3 of Ref. [44]), which can undergo topological phase transitions under certain conditions [8,18,62]. We find that non-Hermitian cooling exists and is almost identical in both topologically trivial and non-trivial phases.

In summary, we proposed a non-Hermitian cooling mechanism that is fundamentally different from traditional refrigeration and laser cooling techniques. The non-Hermitian cooling is generically applicable to various physical systems and can be exponentially enhanced by the number of auxiliary modes. We anticipate the non-Hermitian cooling paradigm to find applications in various domains, such as quantum information science, where efficient cooling towards the ground state is desirable.

We acknowledge support by the Gordon and Betty Moore Foundation's EPiQS Initiative, Grant No. GBMF11945. U. D. acknowledges the support of the Austrian Science Fund (FWF, Project No. I5111-N).

*Corresponding author: pcappell@mit.edu

†Corresponding author: liju@mit.edu

- [1] M. A. Miri and A. Alù, Exceptional points in optics and photonics, *Science* **363**, eaar7709 (2019).
- [2] W. Chen, Ş. Kaya Özdemir, G. Zhao, J. Wiersig, and L. Yang, Exceptional points enhance sensing in an optical microcavity, *Nature (London)* **548**, 192 (2017).
- [3] H. Hodaie, A. U. Hassan, S. Wittek, H. Garcia-Gracia, R. El-Ganainy, D. N. Christodoulides, and M. Khajavikhan, Enhanced sensitivity at higher-order exceptional points, *Nature (London)* **548**, 187 (2017).
- [4] Y. H. Lai, Y. K. Lu, M. G. Suh, Z. Yuan, and K. Vahala, Observation of the exceptional-point-enhanced Sagnac effect, *Nature (London)* **576**, 65 (2019).
- [5] H. Xu, D. Mason, L. Jiang, and J. G. E. Harris, Topological energy transfer in an optomechanical system with exceptional points, *Nature (London)* **537**, 80 (2016).
- [6] Y. Ashida, Z. Gong, and M. Ueda, Non-Hermitian physics, *Adv. Phys.* **69**, 249 (2020).
- [7] E. J. Bergholtz, J. C. Budich, and F. K. Kunst, Exceptional topology of non-Hermitian systems, *Rev. Mod. Phys.* **93**, 015005 (2021).
- [8] S. Yao and Z. Wang, Edge states and topological invariants of non-Hermitian systems, *Phys. Rev. Lett.* **121**, 086803 (2018).
- [9] H. Shen, B. Zhen, and L. Fu, Topological band theory for non-Hermitian Hamiltonians, *Phys. Rev. Lett.* **120**, 146402 (2018).
- [10] K. Kawabata, K. Shiozaki, M. Ueda, and M. Sato, Symmetry and topology in non-Hermitian physics, *Phys. Rev. X* **9**, 041015 (2019).
- [11] Z. Gong, Y. Ashida, K. Kawabata, K. Takasan, S. Higashikawa, and M. Ueda, Topological phases of non-Hermitian systems, *Phys. Rev. X* **8**, 031079 (2018).

- [12] N. Hatano and D.R. Nelson, Vortex pinning and non-Hermitian quantum mechanics, *Phys. Rev. B* **56**, 8651 (1997).
- [13] N. Okuma, K. Kawabata, K. Shiozaki, and M. Sato, Topological origin of non-Hermitian skin effects, *Phys. Rev. Lett.* **124**, 086801 (2020).
- [14] L. Xiao, T. Deng, K. Wang, G. Zhu, Z. Wang, W. Yi, and P. Xue, Non-Hermitian bulk–boundary correspondence in quantum dynamics, *Nat. Phys.* **16**, 761 (2020).
- [15] S. Weidemann, M. Kremer, T. Helbig, T. Hofmann, A. Stegmaier, M. Greiter, R. Thomale, and A. Szameit, Topological funneling of light, *Science* **368**, 311 (2020).
- [16] L. Zhang *et al.*, Acoustic non-Hermitian skin effect from twisted winding topology, *Nat. Commun.* **12**, 6297 (2021).
- [17] X. Zhang, Y. Tian, J. H. Jiang, M. H. Lu, and Y. F. Chen, Observation of higher-order non-Hermitian skin effect, *Nat. Commun.* **12**, 5377 (2021).
- [18] X. Zhang, T. Zhang, M. H. Lu, and Y. F. Chen, A review on non-Hermitian skin effect, *Adv. Phys.* **7**, 2109431 (2022).
- [19] D. S. Borgnia, A. J. Kruchkov, and R. J. Slager, Non-Hermitian boundary modes and topology, *Phys. Rev. Lett.* **124**, 056802 (2020).
- [20] B. Abdo, K. Sliwa, L. Frunzio, and M. Devoret, Directional amplification with a Josephson circuit, *Phys. Rev. X* **3**, 031001 (2014).
- [21] K. M. Sliwa, M. Hatridge, A. Narla, S. Shankar, L. Frunzio, R. J. Schoelkopf, and M. H. Devoret, Reconfigurable Josephson circulator/directional amplifier, *Phys. Rev. X* **5**, 041020 (2015).
- [22] D. Malz, L. D. Tóth, N. R. Bernier, A. K. Feofanov, T. J. Kippenberg, and A. Nunnenkamp, Quantum-limited directional amplifiers with optomechanics, *Phys. Rev. Lett.* **120**, 023601 (2018).
- [23] W. T. Xue, M. R. Li, Y. M. Hu, F. Song, and Z. Wang, Simple formulas of directional amplification from non-Bloch band theory, *Phys. Rev. B* **103**, L241408 (2021).
- [24] H. K. Lau and A. A. Clerk, Fundamental limits and non-reciprocal approaches in non-Hermitian quantum sensing, *Nat. Commun.* **9**, 4320 (2018).
- [25] A. McDonald and A. A. Clerk, Exponentially-enhanced quantum sensing with non-Hermitian lattice dynamics, *Nat. Commun.* **11**, 5382 (2020).
- [26] J. C. Budich and E. J. Bergholtz, Non-Hermitian topological sensors, *Phys. Rev. Lett.* **125**, 180403 (2020).
- [27] D. Porras and S. Fernández-Lorenzo, Topological amplification in photonic lattices, *Phys. Rev. Lett.* **122**, 143901 (2019).
- [28] C. C. Wanjura, M. Brunelli, and A. Nunnenkamp, Topological framework for directional amplification in driven-dissipative cavity arrays, *Nat. Commun.* **11**, 3149 (2020).
- [29] F. Pobell, Matter and methods at low temperatures, *Matter and Methods at Low Temperatures* (Springer Berlin, Heidelberg, 2007).
- [30] D. J. Wineland and W. M. Itano, Laser cooling of atoms, *Phys. Rev. A* **20**, 1521 (1979).
- [31] M. Sheik-Bahae and R. I. Epstein, Laser cooling of solids, *Laser Photonics Rev.* **3**, 67 (2009).
- [32] W. D. Phillips, Nobel lecture: Laser cooling and trapping of neutral atoms, *Rev. Mod. Phys.* **70**, 721 (1998).
- [33] H. Xu, G. Wang, C. Li, H. Wang, H. Tang, A. R. Barr, P. Cappellaro, and J. Li, Laser cooling of nuclear magnons, *Phys. Rev. Lett.* **130**, 063602 (2023).
- [34] H. Xu, L. Jiang, A. A. Clerk, and J. G. E. Harris, Nonreciprocal control and cooling of phonon modes in an optomechanical system, *Nature (London)* **568**, 65 (2019).
- [35] S. A. M. Loos, S. Arabha, A. Rajabpour, A. Hassanali, and É. Roldán, Nonreciprocal forces enable cold-to-hot heat transfer between nanoparticles, *Sci. Rep.* **13**, 1 (2023).
- [36] Y. Wu, W. Liu, J. Geng, X. Song, X. Ye, C. K. Duan, X. Rong, and J. Du, Observation of parity-time symmetry breaking in a single-spin system, *Science* **364**, 878 (2019).
- [37] L. Feng, Z. J. Wong, R. M. Ma, Y. Wang, and X. Zhang, Single-mode laser by parity-time symmetry breaking, *Science* **346**, 972 (2014).
- [38] B. Peng, S. K. Özdemir, F. Lei, F. Monifi, M. Gianfreda, G. L. Long, S. Fan, F. Nori, C. M. Bender, and L. Yang, Parity–time-symmetric whispering-gallery microcavities, *Nat. Phys.* **10**, 394 (2014).
- [39] B. Corzilius, High-field dynamic nuclear polarization, *Annu. Rev. Phys. Chem.* **71**, 143 (2020).
- [40] X. Chen and B. Fan, The emergence of picokelvin physics, *Rep. Prog. Phys.* **83**, 076401 (2020).
- [41] D. C. Brody and E. M. Graefe, Mixed-state evolution in the presence of gain and loss, *Phys. Rev. Lett.* **109**, 230405 (2012).
- [42] H. Y. Yuan, P. Yan, S. Zheng, Q. Y. He, K. Xia, and M. H. Yung, Steady Bell state generation via magnon-photon coupling, *Phys. Rev. Lett.* **124**, 053602 (2020).
- [43] F. Roccati, G. M. Palma, F. Ciccarello, and F. Bagarello, Non-Hermitian physics and master equations, *Open Syst. Inf. Dyn.* **29**, 2250004 (2022).
- [44] See Supplemental Material at <http://link.aps.org/supplemental/10.1103/PhysRevLett.132.110402> for detailed derivations and discussions on the non-Hermitian transition rate and non-Hermitian cooling effect.
- [45] A. Metelmann and A. A. Clerk, Nonreciprocal photon transmission and amplification via reservoir engineering, *Phys. Rev. X* **5**, 021025 (2015).
- [46] A. Kamal, J. Clarke, and M. H. Devoret, Noiseless non-reciprocity in a parametric active device, *Nat. Phys.* **7**, 311 (2011).
- [47] L. Pan, X. Chen, Y. Chen, and H. Zhai, Non-Hermitian linear response theory, *Nat. Phys.* **16**, 767 (2020).
- [48] N. Okuma and M. Sato, Non-Hermitian topological phenomena: A review, *Annu. Rev. Condens. Matter Phys.* **14**, 83 (2023).
- [49] G. G. Pyrialakos, H. Ren, P. S. Jung, M. Khajavikhan, and D. N. Christodoulides, Thermalization dynamics of nonlinear non-Hermitian optical lattices, *Phys. Rev. Lett.* **128**, 213901 (2022).
- [50] K. Fang, J. Luo, A. Metelmann, M. H. Matheny, F. Marquardt, A. A. Clerk, and O. Painter, Generalized non-reciprocity in an optomechanical circuit via synthetic magnetism and reservoir engineering, *Nat. Phys.* **13**, 465 (2017).
- [51] J. Rieser, M. A. Ciampini, H. Rudolph, N. Kiesel, K. Hornberger, B. A. Stickler, M. Aspelmeyer, and U. Delić, Tunable light-induced dipole-dipole interaction between optically levitated nanoparticles, *Science* **377**, 987 (2022).

- [52] Y. G. N. Liu, Y. Wei, O. Hemmatyar, G. G. Pyrialakos, P. S. Jung, D. N. Christodoulides, and M. Khajavikhan, Complex skin modes in non-Hermitian coupled laser arrays, *Light Sci. Appl.* **11**, 1 (2022).
- [53] M. Reisenbauer, H. Rudolph, L. Egyed, K. Hornberger, A. V Zasedatelev, M. Abuzarli, B. A. Stickler, and U. D. Delić, Non-Hermitian Dynamics and Nonreciprocity of Optically Coupled Nanoparticles, [arXiv:2310.02610](https://arxiv.org/abs/2310.02610).
- [54] M. Mariani, F. Deppe, A. Marx, R. Gross, F. K. Wilhelm, and E. Solano, Two-resonator circuit quantum electrodynamics: A superconducting quantum switch, *Phys. Rev. B—Condens. Matter Mater. Phys.* **78**, 104508 (2008).
- [55] Q. Zeng and K. Zeng, Strong phonon-cavity coupling and parametric interaction in a single microcantilever under ambient conditions, *J. Phys. D* **54**, 475307 (2021).
- [56] T. Makihara *et al.*, Ultrastrong magnon–magnon coupling dominated by antiresonant interactions, *Nat. Commun.* **12**, 3115 (2021).
- [57] R. Hisatomi, A. Osada, Y. Tabuchi, T. Ishikawa, A. Noguchi, R. Yamazaki, K. Usami, and Y. Nakamura, Bidirectional conversion between microwave and light via ferromagnetic magnons, *Phys. Rev. B* **93**, 174427 (2016).
- [58] F. Lecocq, L. Ranzani, G. A. Peterson, K. Cicak, R. W. Simmonds, J. D. Teufel, and J. Aumentado, Nonreciprocal microwave signal processing with a field-programmable Josephson amplifier, *Phys. Rev. Appl.* **7**, 024028 (2017).
- [59] A. Ghatak, M. Brandenbourger, J. Van Wezel, and C. Coulais, Observation of non-Hermitian topology and its bulk-edge correspondence in an active mechanical metamaterial, *Proc. Natl. Acad. Sci. U.S.A.* **117**, 29561 (2020).
- [60] J. P. Mathew, J. del Pino, and E. Verhagen, Synthetic gauge fields for phonon transport in a nano-optomechanical system, *Nat. Nanotechnol.* **15**, 198 (2020).
- [61] J. Qian, C. H. Meng, J. W. Rao, Z. J. Rao, Z. An, Y. Gui, and C. M. Hu, Non-Hermitian control between absorption and transparency in perfect zero-reflection magnonics, *Nat. Commun.* **14**, 3437 (2023).
- [62] A. Youssefi, S. Kono, A. Bancora, M. Chegnizadeh, J. Pan, T. Vovk, and T. J. Kippenberg, Topological lattices realized in superconducting circuit optomechanics, *Nature (London)* **612**, 666 (2022).

Supplementary Materials
to
Exponentially Enhanced Non-Hermitian Cooling

Haowei Xu¹, Uroš Delić^{2,3}, Guoqing Wang^{1,3}, Changhao Li^{1,3}, Paola Cappellaro^{1,3,4}, and Ju
Li^{1,5}

¹Department of Nuclear Science and Engineering, Massachusetts Institute of Technology,
Cambridge, Massachusetts 02139, USA

²University of Vienna, Faculty of Physics, Vienna Center for Quantum Science and
Technology, A-1090 Vienna, Austria

³Research Laboratory of Electronics, Massachusetts Institute of Technology, Cambridge,
MA 02139, USA

⁴Department of Physics, Massachusetts Institute of Technology, Cambridge, MA 02139,
USA

⁵Department of Material Science and Engineering, Massachusetts Institute of Technology,
Cambridge, Massachusetts 02139, USA

Table of Contents

1 Non-Hermitian transition rates from the master equation	2
2 Lower bound of the non-Hermitian cooling effect	4

1 Non-Hermitian transition rates from the master equation

In this section, we demonstrate how one can obtain the non-Hermitian transition rates from the master equation. We will focus a two-mode systems with the same intrinsic frequency ω_0 . Using the rotating wave approximation, the Hamiltonian can be written as

$$\mathcal{H} = t_{12}a_1a_2^\dagger + t_{21}a_1^\dagger a_2, \quad (\text{S1})$$

where $t_{12} = te^A$ and $t_{21} = te^{-A}$ indicate non-Hermitian interaction with $A \neq 0$ a real number. The master equation for a non-Hermitian system can be expressed as [1]

$$\frac{\partial \rho}{\partial t} = -i(\mathcal{H}\rho - \rho\mathcal{H}^\dagger) + i\text{Tr}\{\rho(\mathcal{H} - \mathcal{H}^\dagger)\}\rho + \sum_i \mathcal{L}(\zeta_i)\rho, \quad (\text{S2})$$

where $\text{Tr}\{o\}$ is the trace of operator o . Compared with the standard master equation, the first term in Eq. (S2) is adapted to a non-Hermitian Hamiltonian $\mathcal{H} \neq \mathcal{H}^\dagger$. In practice, there are different approaches to achieve the non-Hermiticity $t_{21} \neq t_{12}$, such as reservoir engineering [2] or parametric driving [3, 4]. These are *controlled and desired* interactions with certain external modes, and we (approximately) incorporate them using the non-Hermitian Hamiltonian. The second term in Eq. (S2) is used to make the master equation trace conserving (i.e., to maintain $\text{Tr}\{\rho\} = 1$) [1]. Meanwhile, the third term, $\mathcal{L}(\zeta_i)\rho \equiv \zeta_i\rho\zeta_i^\dagger - \frac{1}{2}\zeta_i^\dagger\zeta_i\rho - \frac{1}{2}\rho\zeta_i^\dagger\zeta_i$, is the Lindblad operator, which represents the *uncontrolled and undesired* dissipative interaction with the environment.

For the two-mode system under consideration, one needs to include four ζ operators, namely,

$$\begin{aligned} \zeta_1 &= \sqrt{\kappa_1(n_{\text{th}} + 1)}a_1, \\ \zeta_2 &= \sqrt{\kappa_1 n_{\text{th}}}a_1^\dagger, \\ \zeta_3 &= \sqrt{\kappa_2(n_{\text{th}} + 1)}a_2, \\ \zeta_4 &= \sqrt{\kappa_2 n_{\text{th}}}a_2^\dagger, \end{aligned} \quad (\text{S3})$$

where $\kappa_{1(2)}$ and n_{th} are the thermal dissipation rate and the thermal occupation number, respectively.

Then, we need to obtain how the occupation number of each mode evolves with time. For mode-1,

we need to calculate

$$\frac{\partial \langle a_1^\dagger a_1 \rangle}{\partial t} = \frac{\partial}{\partial t} \text{Tr} \left\{ \rho a_1^\dagger a_1 \right\} = \text{Tr} \left\{ \frac{\partial \rho}{\partial t} a_1^\dagger a_1 \right\}. \quad (\text{S4})$$

Here $\langle o \rangle \equiv \text{Tr} \{ \rho o \}$ is the thermal average of operator o . From Eq. (S2), one can see that $\frac{\partial \rho}{\partial t}$ is composed of three parts. The first part, which comes from the first term on the right hand side of Eq. (S2), can be expressed as

$$\begin{aligned} \left[\frac{\partial \langle a_1^\dagger a_1 \rangle}{\partial t} \right]_{(1)} &= -i \text{Tr} \left\{ (\mathcal{H} \rho - \rho \mathcal{H}^\dagger) a_1^\dagger a_1 \right\} \\ &= i \langle \mathcal{H}^\dagger a_1^\dagger a_1 - a_1^\dagger a_1 \mathcal{H} \rangle \\ &= i \langle t_{12}^* a_1^\dagger a_2 a_1^\dagger a_1 + t_{21}^* a_1 a_2^\dagger a_1^\dagger a_1 - t_{12} a_1^\dagger a_1 a_1 a_2^\dagger + t_{21} a_1^\dagger a_1 a_1^\dagger a_2 \rangle. \end{aligned} \quad (\text{S5})$$

Here we assume that the occupations of the two modes are both very small, so that the two-operator averages such $\langle a_1^\dagger a_1 \rangle$ and $\langle a_2^\dagger a_2 \rangle$ are much smaller than 1. Consequently, to the first order of two-operator averages, some four-operator averages such as $\langle a_1^\dagger a_2 a_1^\dagger a_1 \rangle$ can be ignored because one has $\langle a_1^\dagger a_2 a_1^\dagger a_1 \rangle \sim \langle a_1^\dagger a_2 \rangle \langle a_1^\dagger a_1 \rangle \ll \langle a_1^\dagger a_2 \rangle$ [5]. This approximation leads to

$$\left[\frac{\partial \langle a_1^\dagger a_1 \rangle}{\partial t} \right]_{(1)} \approx i \left[t_{12} \langle a_1 a_2^\dagger \rangle - t_{21} \langle a_1^\dagger a_2 \rangle \right]. \quad (\text{S6})$$

Similarly, the contributions from the second and third terms on the right hand side of Eq. (S2) are

$$\begin{aligned} \left[\frac{\partial \langle a_1^\dagger a_1 \rangle}{\partial t} \right]_{(2)} &\approx 0, \\ \left[\frac{\partial \langle a_1^\dagger a_1 \rangle}{\partial t} \right]_{(3)} &= -\kappa_1 \left[\langle a_1^\dagger a_1 \rangle - n_{\text{th}} \right]. \end{aligned} \quad (\text{S7})$$

Finally, one has

$$\begin{aligned} \frac{\partial \langle a_1^\dagger a_1 \rangle}{\partial t} &= \left[\frac{\partial \langle a_1^\dagger a_1 \rangle}{\partial t} \right]_{(1)} + \left[\frac{\partial \langle a_1^\dagger a_1 \rangle}{\partial t} \right]_{(2)} + \left[\frac{\partial \langle a_1^\dagger a_1 \rangle}{\partial t} \right]_{(3)} \\ &\approx i \left[t_{12} \langle a_1 a_2^\dagger \rangle - t_{21} \langle a_1^\dagger a_2 \rangle \right] - \kappa_1 \left[\langle a_1^\dagger a_1 \rangle - n_{\text{th}} \right]. \end{aligned} \quad (\text{S8})$$

The time evolution of other two-operator averages can be obtained in a similar fashion, and one has

$$\begin{aligned} \frac{\partial \langle a_2^\dagger a_2 \rangle}{\partial t} &\approx i \left[t_{21} \langle a_1^\dagger a_2 \rangle - t_{12} \langle a_1 a_2^\dagger \rangle \right] - \kappa_2 \left[\langle a_2^\dagger a_2 \rangle - n_{\text{th}} \right], \\ \frac{\partial \langle a_1^\dagger a_2 \rangle}{\partial t} &\approx i \left[t_{21}^* \langle a_2^\dagger a_2 \rangle - t_{12} \langle a_1^\dagger a_1 \rangle \right] - \frac{\kappa_1 + \kappa_2}{2} \langle a_1^\dagger a_2 \rangle, \\ \frac{\partial \langle a_1 a_2^\dagger \rangle}{\partial t} &\approx i \left[t_{12}^* \langle a_1^\dagger a_1 \rangle - t_{21} \langle a_2^\dagger a_2 \rangle \right] - \frac{\kappa_1 + \kappa_2}{2} \langle a_1 a_2^\dagger \rangle. \end{aligned} \quad (\text{S9})$$

In the steady state, all time derivatives can be set to zero, yielding

$$\begin{aligned} g_{12}n_1 + \kappa_1 n_1 &= g_{21}n_2 + \kappa_1 n_{\text{th}}, \\ g_{21}n_2 + \kappa_2 n_2 &= g_{12}n_1 + \kappa_2 n_{\text{th}}, \end{aligned} \tag{S10}$$

where

$$\begin{aligned} g_{12} &= \frac{2(|t_{12}|^2 + t_{12}t_{21})}{\kappa_1 + \kappa_2}, \\ g_{21} &= \frac{2(|t_{21}|^2 + t_{12}t_{21})}{\kappa_1 + \kappa_2} \end{aligned} \tag{S11}$$

are the non-reciprocal transition rates between modes 1 and 2. Notably, when $t_{12} = t_{21} = t$, one has $g_{12} = g_{21} = \frac{4t^2}{\kappa_1 + \kappa_2}$, a well-known result that can be obtained from Fermi's golden rule.

2 Lower bound of the non-Hermitian cooling effect

In the main text, we mentioned that the steady-state occupation of the principal mode can be made exponentially small by adding more auxiliary modes, but there is a lower-bound when the dissipative interaction with the environment is considered. This lower-bound can be obtained by examining the steady-state equation of mode-1 in the N -mode non-Hermitian chain, which is

$$\begin{aligned} g_{12}n_1 + \kappa n_1 &= g_{21}n_2 + \kappa n_{\text{th}} \\ \implies n_1 &= \frac{g_{21}n_2 + \kappa n_{\text{th}}}{g_{12} + \kappa}. \end{aligned} \tag{S12}$$

Clearly, n_1 can be minimized when n_2 is minimized. However, one always has $n_2 > n_1$ no matter how long the non-Hermitian chain is. Hence, the lower bound for n_1 can be obtained by setting $n_2 = n_1$ in Eq. (S12), yielding

$$\begin{aligned} \lim_{N \rightarrow \infty} n_1(N, \kappa) &\approx \frac{\kappa n_{\text{th}}}{\kappa + g_{12} - g_{21}} \\ &= \frac{\kappa^2 n_{\text{th}}}{\kappa^2 + t_{12}^2 - t_{21}^2}. \end{aligned} \tag{S13}$$

This result is plotted as the dashed curve in Figure S1, which exhibits reasonable agreement with the results obtained by numerically solving the steady-state equation in the main text with a very large N (red circles). Similar agreements have been found for the non-Hermitian chain with different e^A (Figure S2).

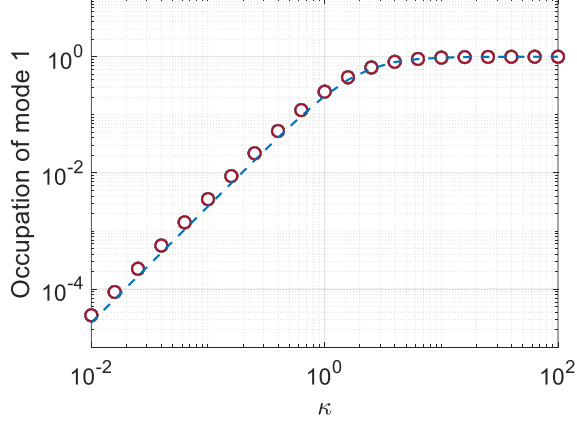


Figure S1: The lower bound of the steady-state occupation of mode-1 in the non-Hermitian chain with $e^A = 2$. The blue dashed curve comes from Eq. (S12), while the red circles are obtained by numerically solving the steady-state equation with a very large $N = 100$.

3 Non-Hermitian cooling in the Su–Schrieffer–Heeger model

In the main text, we used the Hatano-Nelson model to demonstrate the non-Hermitian cooling effect. The Hatano-Nelson model does not exhibit exceptional points or topological properties. Here, we investigate the non-Hermitian cooling effect in the non-Hermitian Bosonic Su–Schrieffer–Heeger (SSH) model, which can undergo topological phase transitions.

In the SSH model, one unit cell i is composed of two modes labelled by A and B , respectively [Figure S3(a)]. For a N -unit-cell SSH chain, the Hamiltonian can be expressed as

$$\begin{aligned} \mathcal{H} = & \sum_{i=1}^N t_1 \left(a_{i,A} a_{i,B}^\dagger + a_{i,A}^\dagger a_{i,B} \right) \\ & + \sum_{i=1}^{N-1} (t_2 + \gamma) a_{i+1,A}^\dagger a_{i,B} + (t_2 - \gamma) a_{i+1,A} a_{i,B}^\dagger. \end{aligned} \quad (\text{S14})$$

One can see that the chain is non-Hermitian when γ is a non-zero real number. In the Hermitian SSH model with $\gamma = 0$, the topological phase transition happens at $t_1 = t_2$. In the non-Hermitian SSH model with $\gamma \neq 0$, the topological phase transition point is influenced by γ [6]. In the following, we will fix $N = 20$ and $\gamma = 0.3t_2$. The numerical spectra of the SSH model are shown in Figure S3(b), where one can observe a topological phase transition when $t_1 \approx 0.7t_2$.

Then, we study the non-Hermitian cooling effect using $t_2 = 0.5t_1$ and $t_2 = 1.5t_1$, whereby the SSH model belongs to different topological phases [dashed vertical lines in Figure S3(b)]. The results are shown in Figure S4. One can see that the non-Hermitian cooling effect is almost identical in the two

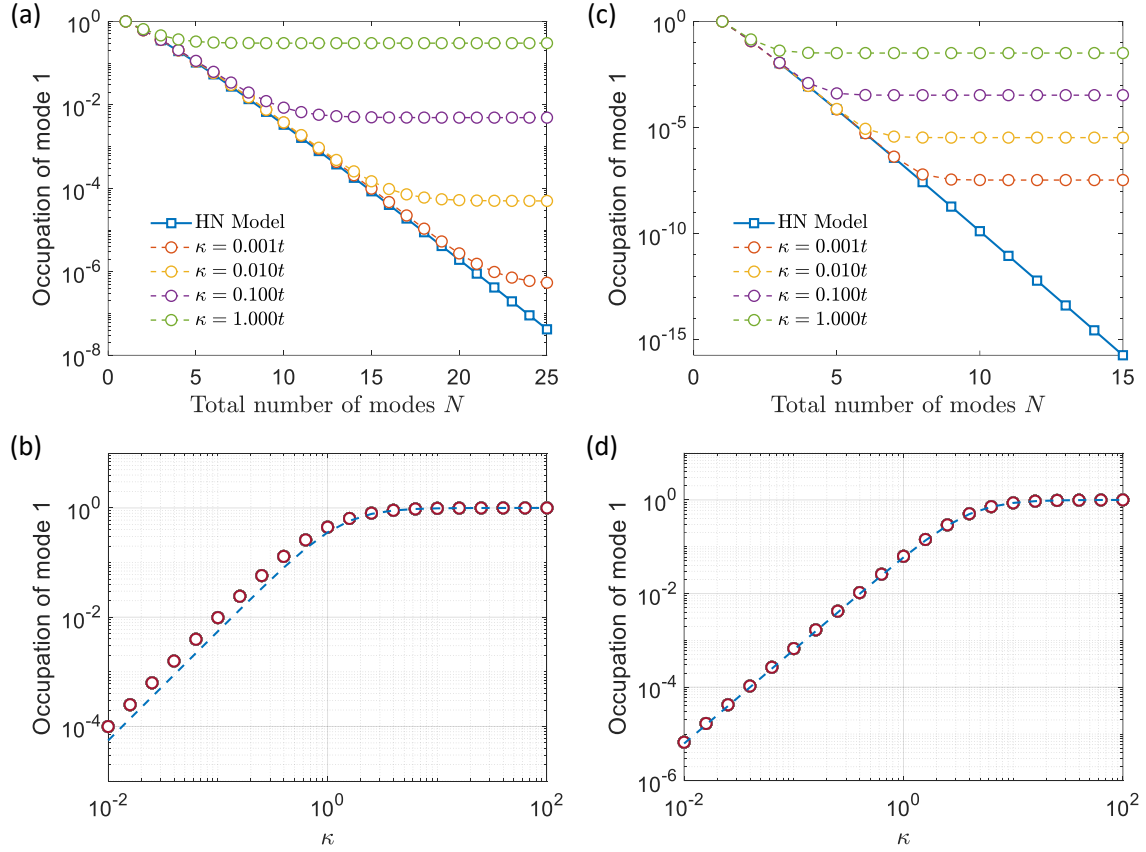


Figure S2: (a,c) Steady-state occupation of the mode-1 as a function of N with varying κ . The solid blue line are obtained from the wavefunctions of the Hatano-Nelson model, while the circles are obtained by solving the steady-state equations. (b,d) The lower bound of the steady-state occupation of mode-1 in the non-Hermitian chain. The labels are the same as those in Figure S1. e^A is set as 1.5 and 4 in (a,b) and (c,d), respectively.

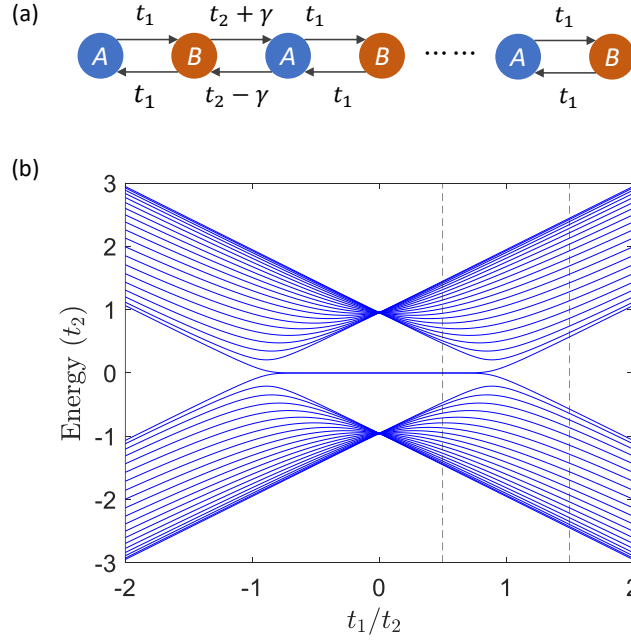


Figure S3: (a) An illustration of the SSH model. (b) Numerical spectra of the SSH model with $N = 20$ and $\gamma = 0.3t_2$.

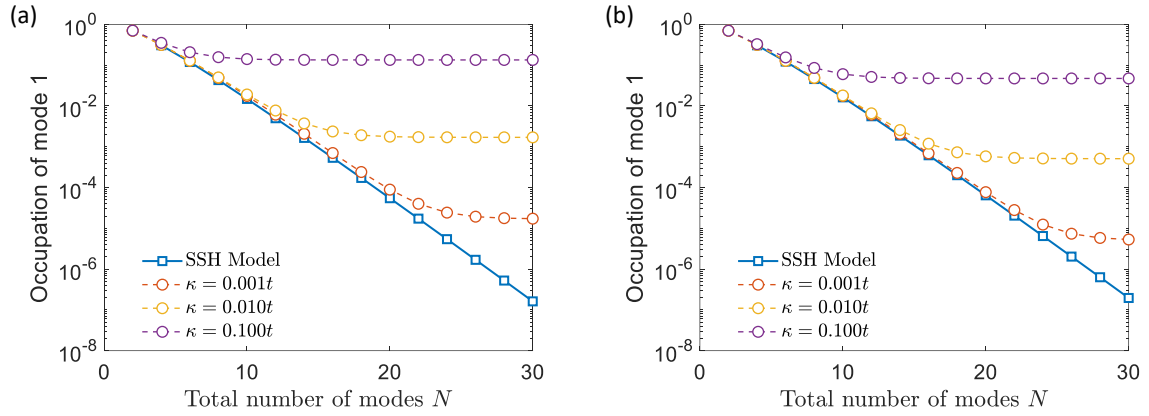


Figure S4: Steady-state occupation of the mode-1 as a function of N with varying κ in the SSH model. The solid blue lines are obtained from the wavefunctions of the SSH model, while the circles are obtained by solving the steady-state equations.

phases. Moreover, the predictions from the wavefunction density (solid blue lines) agree with the results from the steady-state equations in the limit of $\kappa \rightarrow 0$. These results suggest that the non-Hermitian cooling effect does not require non-trivial topology.

4 Reservoir engineering under finite temperature

Reservoir engineering [2] is one of the most popular approaches to generating non-Hermitian interactions. Here an engineered auxiliary reservoir is used to generate non-Hermitian interactions between two modes labelled by 1 and 2, respectively. The engineered reservoir needs to *coherently* absorb quanta from (or emit quanta to) the two modes. In the original work [2], the authors considered a zero-temperature reservoir, whose thermal occupation is thus zero. In this case, the authors only included one jump operator $z = d_1 + d_2$, which describes the interaction between the reservoir and the two-modes. Here d_i is the annihilation operator of the i -th mode (see texts around Eq. (8) in Ref. [2]).

Here we generalize the discussions in Ref. [2], and consider a reservoir with finite temperature and thus finite occupation number n_0 . In this case, we need to consider two jump operators

$$\begin{aligned} z_1 &= \sqrt{n_0 + 1}(d_1 + d_2) \\ z_2 &= \sqrt{n_0}(d_1^\dagger + d_2^\dagger) \end{aligned} \tag{S15}$$

Note that the zero-temperature case considered in Ref. [2] corresponds to $n_0 = 0$. Then, we still consider the master equation

$$\frac{\partial}{\partial t}\rho = -i[\mathcal{H}_{\text{hop}}, \rho] + \Gamma \sum_{i=1,2} \mathcal{L}(z_i)\rho + \kappa \sum_{j=1,2} \mathcal{L}(d_j)\rho \tag{S16}$$

Here $\mathcal{H}_{\text{hop}} = Jd_1^\dagger d_2 + h.c.$ is the coherent interaction between modes 1 and 2, with J the coupling strength. *h.c.* stands for Hermitian conjugate. The second term in Eq. (S16) is the interaction with the engineered reservoir at rate Γ , while the last term describes the interaction between the two modes and their input-out ports at rate κ . More detailed discussions can be found in Ref. [2].

After some tedious but straightforward derivations, one will find that

$$\begin{aligned} \frac{\partial}{\partial t}\langle d_1 \rangle &\equiv \frac{\partial}{\partial t}\text{Tr}\{\rho d_1\} = -\frac{\kappa + \Gamma}{2}\langle d_1 \rangle - \left[iJ + \frac{\Gamma}{2} \right] \langle d_2 \rangle, \\ \frac{\partial}{\partial t}\langle d_2 \rangle &\equiv \frac{\partial}{\partial t}\text{Tr}\{\rho d_2\} = -\frac{\kappa + \Gamma}{2}\langle d_2 \rangle - \left[iJ^* + \frac{\Gamma}{2} \right] \langle d_1 \rangle. \end{aligned} \tag{S17}$$

This is exactly the same as Eq. (10) in Ref. [2], which is the key result there. In other words, the

non-Hermitian interaction generated by reservoir engineering remains the same, regardless of whether the reservoir has finite thermal occupation n_0 .

The fluctuation of the thermal occupation can be included by using a time-dependent $n_0(t) = \langle n_0 \rangle + \delta n_0(t)$, where $\langle n_0 \rangle$ is the average occupation, while $\delta n_0(t)$ is a fluctuation (noise). Even in this case, one can still obtain Eq. (S17), where $n_0(t)$ does not appear. Indeed, the noise term $\delta n_0(t)$ could influence the dynamics as second-order or even higher-order perturbations, but these effects should be quite weak¹. A systematic analysis on these effects is beyond the scope of the current work and will be left for future studies.

References

- [1] Brody, D. C. & Graefe, E.-M. Mixed-state evolution in the presence of gain and loss. *Physical review letters* **109**, 230405 (2012).
- [2] Metelmann, A. & Clerk, A. A. Nonreciprocal photon transmission and amplification via reservoir engineering. *Physical Review X* **5**, 021025 (2015).
- [3] Sliwa, K. *et al.* Reconfigurable josephson circulator/directional amplifier. *Physical Review X* **5**, 041020 (2015).
- [4] Kamal, A., Clarke, J. & Devoret, M. Noiseless non-reciprocity in a parametric active device. *Nature Physics* **7**, 311–315 (2011).
- [5] Pan, L., Chen, X., Chen, Y. & Zhai, H. Non-hermitian linear response theory. *Nature Physics* **16**, 767–771 (2020).
- [6] Yao, S. & Wang, Z. Edge states and topological invariants of non-hermitian systems. *Physical review letters* **121**, 086803 (2018).

¹This might be especially true when $\langle n_0 \rangle$ is large, so that the relative variance $\sqrt{\langle \delta n_0^2(t) \rangle} / \langle n_0 \rangle$ is small